International Journal of Automotive Technology, Vol. 9, No. 2, pp. 183−190 (2008)
DOI 10.1007/s12239−008−0023−8

1229−9138/2008/039−08

NEW NONLINEAR BUSHING MODEL FOR GENERAL EXCITATIONS USING BOUC-WEN HYSTERETIC MODEL

J. K. OK[1)], W. S. YOO[1)] and J. H. SOHN[2)*]

[1)]School of Mechanical Engineering, Pusan National University, Busan 609-735, Korea
[2)]School of Mechanical Engineering, Pukyong National University, Busan 608-739, Korea

(Received 10 August 2007; Revised 21 November 2007)

ABSTRACT−Because the characteristics of rubber bushing significantly affect the accuracy of vehicle dynamics simulations, they should be accurately modeled in the vehicle suspension model. In this paper, a new nonlinear bushing model for automotive bushing components is developed to improve the accuracy of vehicle dynamics analysis. Bushing components were first tested to capture the nonlinear and hysteretic behavior of typical elements by using a MTS 3-axis elastomer tester. A simple Bouc-Wen hysteretic differential model was modified to generate a more precise rubber bushing model. A sine wave, step input, and random excitations are imposed on the bushing. The ADAMS program is used to calculate sensitivity and the VisualDOC program is employed to find the optimal parameters for the bushing model. An error function is designed to find optimal parameters of the model. Parameter identification is carried out to satisfy the static and dynamic characteristics due to sine and step excitation inputs. It was proved that the proposed model could predict the bushing forces under sine, step, and random inputs well. The errors are within 10% in the overall range. To show the validity of the proposed model, a numerical example was also carried out. Because the bushing forces due to random excitation input show good agreement with experiments, the proposed bushing model is available in the vehicle dynamics simulation.

KEY WORDS : Vehicle dynamics analysis, Rubber bushing, Suspension system, Hysteresis

1. INTRODUCTION

A vehicle suspension model should take into account rubber bushing effects because they significantly affect the accuracy of the vehicle dynamics simulation. Because of the rubber materials in the bush, the bushing element has nonlinear characteristics for both load amplitudes and frequencies in addition to hysteretic responses for repeated vibrational excitations. Blundell (1998) used a joint model, a linear bushing model, and a nonlinear bushing model to describe the influence of rubber bush compliance on vehicle suspension movements. The multibody dynamic analysis programs such an ADAMS (MSC Software Corporation, 2005) and RecurDyn (FunctionBay, Inc., 2006) adopt the Kelvin-Voight model for the bushing element. This model represents the bushing element as the linear combination of three translational spring-dampers and three rotational spring-dampers. This type of bushing model cannot generate the nonlinear hysteretic behavior of the bushing element.

The Bouc-Wen model has been widely used to represent non-linear hysteretic systems. The Bouc-Wen differential model was originally proposed by Bouc (1967) and modified by Wen (1975). This nonlinear differential equation model includes the time-history-dependent nature of the hysteretic force. For a given time history of the displacement, the restoring force is completely specified by the differential model, without need for empirical rules or additional conductions. Sain *et al.* (1998) carried out an initial study of qualitative characteristics, and Ni *et al.* (1998) studied the identification of non-linear hysteretic isolators from periodic vibration tests. Spencer *et al.* (1997) developed the phenomenological model of a magnetorheological damper.

Yoo *et al.* (2004) suggested an artificial neural network bushing model for considering the nonlinear hysteretic behaviors of the bushing. Ok *et al.* (2005) employed a simple Bouc-Wen hysteretic model for bushing modeling. In those experiments, a sine excitation input test was carried out using the MTS one-axis durability tester and test results were used to develop the bushing model.

In this paper, the Bouc-Wen model is modified to develop a new bushing model. The proposed model can control the stiffness and damping coefficients by properly setting the design parameters. The ADAMS program is used for modeling and dynamic analysis, and VisualDOC (Vanderplaats Research & Development, Inc., (2006) program is employed to find the optimal parameters. The experimental setup and test results are briefly explained in section 2. A new bushing model using Bouc-Wen hysteretic model is proposed in section 3, and the parameter identification procedures are explained in section 4. The numerical examples

**Corresponding author.* e-mail: jhsohn@pknu.ac.kr

are shown in section 5, and finally, conclusions and suggestions are in section 6.

2. EXPERIMENTS FOR RUBBER BUSHING CHARACTERISTICS

The configuration of the bushing and an MTS 3-axis elastomer testing system used in this paper are shown in Figure 1 and Figure 2, respectively. The test procedure is well explained in the paper by Ok *et al.* (2007).

Harmonic, step, and random input tests were carried out, and some typical test results are shown in Figure 3, Figure 4, and Figure 5.

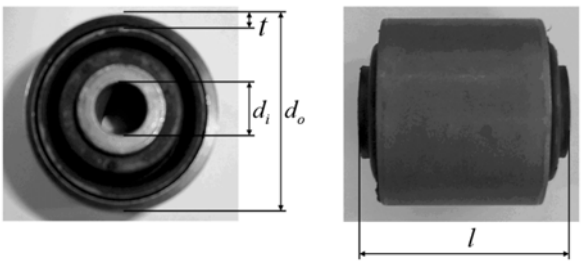

Figure 1. Bushing configuration.

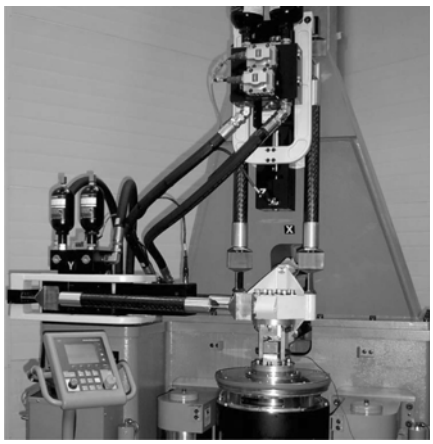

Figure 2. 3-axis elastomer testing system.

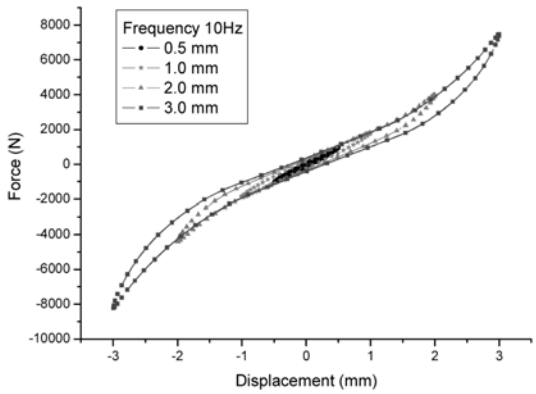

Figure 3. Bushing forces due to amplitude changes.

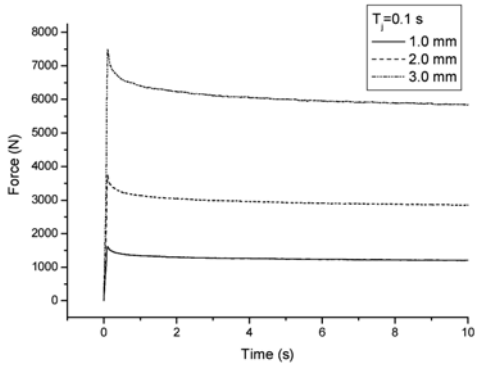

Figure 4. Bushing forces according to amplitude changes (step input with rise time of 0.1 s).

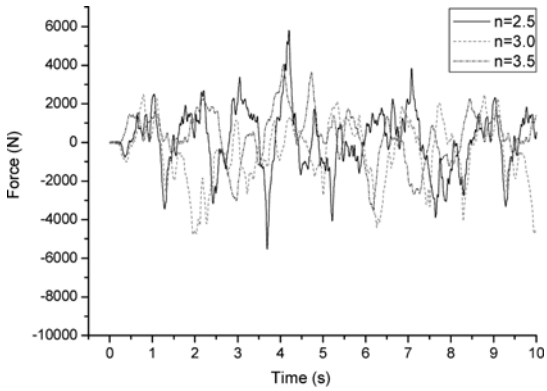

Figure 5. Bushing forces due to random excitations.

3. NEW BUSHING MODELING USING BOUC-WEN HYSTERETIC MODEL

3.1. Previous Bushing Models

3.1.1. Bouc-Wen model

The Bouc-Wen model, as shown in Figure 6, is composed of spring element (k_0), damping component (c_0), and the hysteretic loop in parallel. There are two types of models, the nonparametric model and parametric model. For the nonparametric model, it is easy to find the coefficients, but

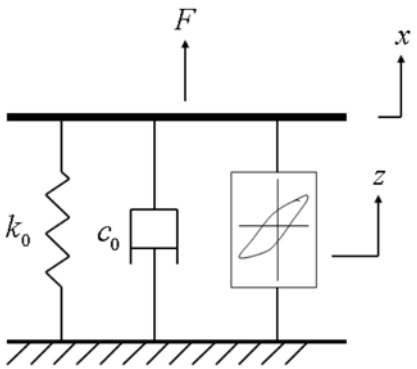

Figure 6. Bouc-Wen hysteretic model.

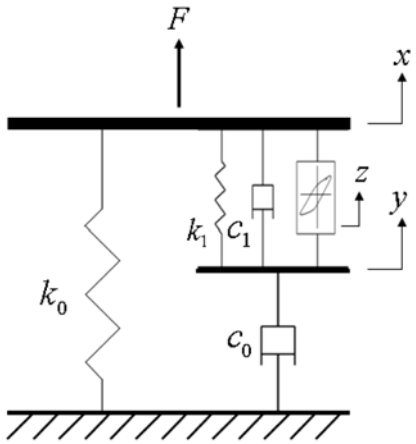

Figure 7. Spencer model for the MR damper.

they can not be verified in terms of reliability and adaptation. Parametric models with the Bouc-Wen model can overcome this problem (Sues *et al*., 1988).

3.1.2. Spencer model

To better predict the hysteretic response, a modified version of the Bouc-Wen model was proposed by Spencer (1997), which is shown in Figure 7. It is a second-order dynamic linear model with an embedded sophisticated hysteretic (non-linear) model. In addition to the Bouc-Wen model, an additional spring element (k_1) and a damping component (c_1) were included to consider the nonlinear characteristics of the MR damper.

3.2. A New Bushing Model

Although Spencer employed the Bouc-Wen model to predict the responses of the MR damper, his model just captured the damper response including velocity relationship. However, a more general bushing model is required to capture not only the velocity but also the displacement.

In this paper, the Spencer model is modified to be used in the bushing modeling of the vehicle suspension. As shown in Figure 8, another Bouc-Wen model is added to the spring element to take into account the nonlinear characteristics with respect to displacement. As shown in Figure 8, the left term of the proposed model is composed of the standard solid model and the Bouc-Wen model to represent the nonlinearity of the bushing stiffness. The right term is composed of the linear damper and the Bouc-Wen model to represent the hysteretic characteristics.

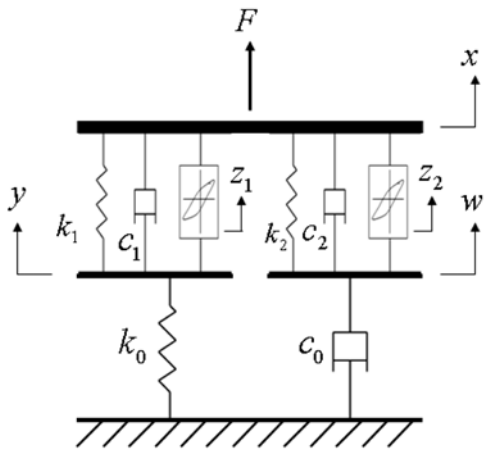

Figure 8. Proposed model of the bushing.

Bushing forces for the new model shown in Figure 8 can be calculated from the following equations, where x, y, and w are displacement of the upper plate, the lefthand plate, and the righthand plate, respectively. In Figure 8, k_0 and k_1 represent the bushing stiffness and c_1 is the parameter which accounts for the relaxation of the bushing impact force. The parameter z_1 is the imaginary hysteretic force to represent the linear hysteretic characteristics of the bushing. The parameter c_2 represents the the viscous damping observed at large velocities. A dashpot, c_0, produces the roll-off observed in the experimental data at low velocities. The parameter k_2 is used to control the stiffness at large velocities, and finally, z_2 is the imaginary hysteretic force to represent the nonlinear hysteretic characteristics of the bushing.

$$\dot{z}_1=(\dot{x}-\dot{y})[A_1-\{\gamma_1+\beta_1\mathrm{sgn}(\dot{x}-\dot{y})\mathrm{sgn}(z_1)\}|z_1|^{n_1}] \quad (1)$$

$$\dot{z}_2=(\dot{x}-\dot{w})[A_2-\{\gamma_2+\beta_2\mathrm{sgn}(\dot{x}-\dot{w})\mathrm{sgn}(z_2)\}|z_2|^{n_2}] \quad (2)$$

$$\dot{y}=\frac{1}{c_1}\{c_1\dot{x}+k_1(x-y)-k_o y+\alpha_1 z_1\} \quad (3)$$

$$\dot{w}=\frac{1}{c_o+c_2}\{c_2\dot{x}+k_2(x-w)+\alpha_2 z_2\} \quad (4)$$

$$F(t)=k_o y+c_o\dot{w} \quad (5)$$

4. PARAMETER IDENTIFICATION FOR PROPOSED MODEL

For the proposed bushing model, parameters are adjusted for a sinusoidal input, a step input and a combination of sine and step inputs.

4.1. Identification from Sine Input

The periodic excitation input is often applied to the suspension bushing when the vehicle runs over a road. In this section, the parameters of the proposed model are obtained for periodic input for the bushing.

4.1.1. Sensitivity analysis to sine input

Sensitivity analysis to harmonic excitation is carried out to know how the parameters affect the bushing forces. Local sensitivity analysis in the ADAMS program is employed, in which one parameter is repeatedly changed while the others maintain chosen values. The objective function for sensitivity analysis used in this paper is written in equation (6) (Atkinson and Han, 2004).

Table 1. Priority of parameters under sine input.

Parameter	Significance priority	Parameter	Significance priority
c_o	11	c_2	12
k_o	3	k_2	16
β_1	13	β_2	6
γ_1	15	γ_2	2
n_1	10	n_2	1
α_1	8	α_2	4
c_1	14	A_1	9
k_1	5	A_2	7

$$E_1=\frac{1}{m}\sum_{i=1}^{m}(F_{\exp}-F_{pre})^2$$

subject to (6)

$$A_{1,2}\geq 1,\ \beta_{1,2}\geq 0,\ \beta_1+\gamma_1>0,\ \beta_2-\gamma_2>0$$

where $F_{\exp}$ is the bushing force obtained from experiments, F_{pre} is from the simulation, and m is the number of data points.

The results of the sensitivity analysis are shown in Table 1. The parameters, n_2, γ_2 and k_o are the most effective in controlling the hysteretic shape of the proposed model. Both α_2 and k_1 also showed a considerable contribution.

4.1.2. Parameter identification from sine input

The parameter identification is carried out by minimizing the root mean square (RMS) error E_1 in equation (6). The VisualDOC program, which is a general-purpose optimization tool that allows the user to quickly apply design optimization capabilities, is employed to minimize RMS error. To optimize the parameters, a genetic algorithm is employed in this paper. The genetic algorithm is known as the proper method to optimize a nonlinear system. To use the genetic algorithm in the VisualDOC program, the population size, the maximum number of iterations, and probability of mutation were chosen to be 300, 200 and 0.05, respectively. The crossover type is assumed to be uniform and the probability of crossover is assigned as 0.8. A sine excitation with an amplitude 2.0 mm and a frequency of 10 Hz is used to perform the parameter identification and the results are shown in Table 2. Bushing forces, measured and predicted, are shown and compared in Figure 9. The results show good agreements with experiments.

Table 2. Parameter values obtained from the identification (sine input).

Parameter	Opt. value	Parameter	Opt. value
c_o	256.358	c_2	0.835
k_o	2417.855	k_2	3.343
β_1	14.220	β_2	1.416
γ_1	−6.155	γ_2	−5.332
n_1	0.426	n_2	0.850
α_1	0.532	α_2	0.913
c_1	4.308	A_1	2473.783
k_1	2007.600	A_2	32.246

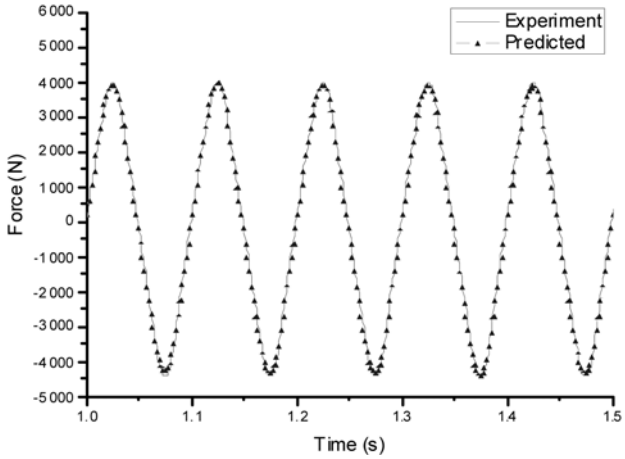

Figure 9. Bushing forces due to sine input.

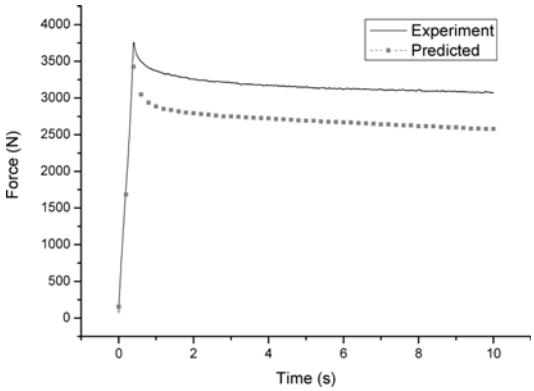

Figure 10. Bushing forces due to step input using the parameters identified through the sine input.

To verify the applicability of identification results with sinusoidal input to a step input, a step input with 2.0 mm of displacement and 0.4 s of rise time is imposed on the bushing. When the bushing forces shown in Figure 10 were applied to the identified result for a sine input, the difference between the experiment and the simulation was 325 N. Thus, the parameters for sinusoidal input can not be applied to a step input.

4.2. Identification from Step Input

4.2.1. Sensitivity analysis to step input

When the step input is imposed on the bushing, the forces exerted on the proposed model shown can be represented by Figure 11. As shown in Figure 11(a), the bushing force reaches its peak and then decreases linearly due to the

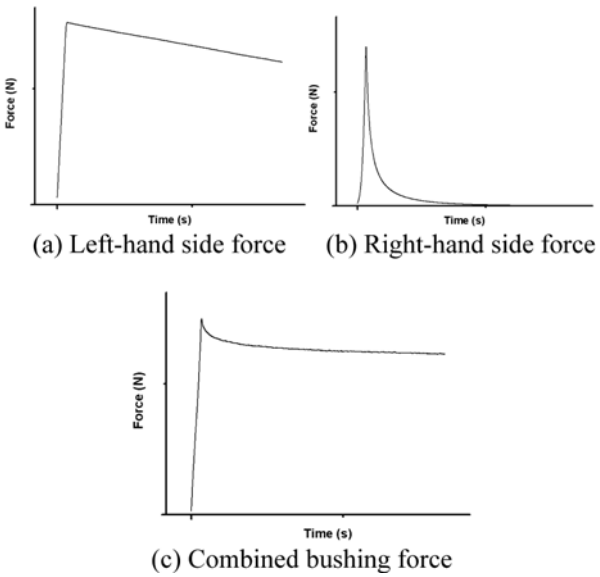

Figure 11. Force mechanism of a proposed bushing model under step input.

Table 3. Priority of parameters under step input.

Parameter	Significance priority		Parameter	Significance priority	
	$t=T_j^*$	$t=10$s		$t=T_j^*$	$t=10$s
c_o	7	10	c_2	14	9
k_o	1	1	k_2	15	11
β_1	10	6	β_2	12	12
γ_1	11	7	γ_2	6	13
n_1	13	3	n_2	4	15
α_1	2	4	α_2	8	14
c_1	16	8	A_1	3	2
k_1	5	5	A_2	9	16

parameter c_1. In Figure 11(b), the bushing force reaches the peak and then rapidly decreases due to combining the parameter c_0 with c_2. Finally, the bushing forces can be shown as in Figure 11(c).

To consider the responses due to the step input, the maximum bushing force and relaxation phenomenon must be included. The objective function used in this paper can be written by the equation (7).

$$E_2=(F_{\exp}-F_{pre})_{t=T_j^*} \tag{7a}$$

$$E_2=(F_{\exp}-F_{pre})_{t=10s} \tag{7b}$$

The right hand side of equation (7a) represents the bushing force difference between the experiment and simulation at the rise time. The right hand side of the equation (7b) is the difference of the bushing force between experiment and simulation at t = 10 s.

The results of the sensitivity analysis are shown in Table 3. The parameters k_0 and k_1 are the important parameters and n_2, γ_2, and α_2 have lower sensitivity than the sine excitation input. This is because the response to step input is a little affected by the shape of the hysteretic curve.

Table 4. Parameter values obtained from the identification (step input).

Parameter	Opt. value	Parameter	Opt. value
c_o	167.204	c_2	2.455
k_o	2380.163	k_2	10.666
β_1	10.938	β_2	0.324
γ_1	−9.987	γ_2	−3.295
n_1	0.430	n_2	0.819
α_1	1.161	α_2	2.108
c_1	1.579	A_1	2378.766
k_1	2133.353	A_2	30.965

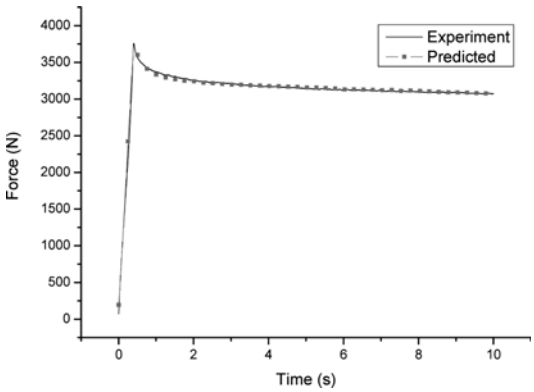

Figure 12. Bushing forces due to step input after identification through step input.

4.2.2. Parameter identification from step input

The parameter identification in response to step input is carried out by using the same displacement as the sine input 2.0 mm and 0.4 s rise time is used. Table 4 shows the parameters obtained from the identification process. The bushing forces resulting from step input after identification

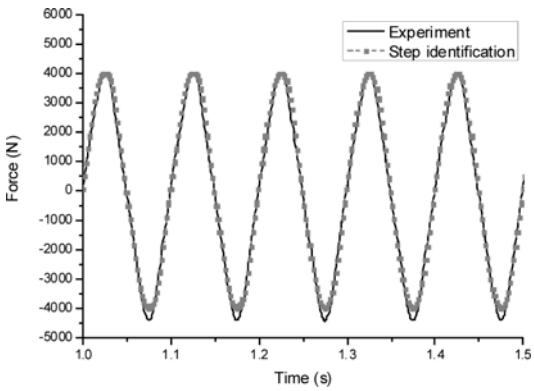

Figure 13. Bushing forces due to sine input after identification through step input.

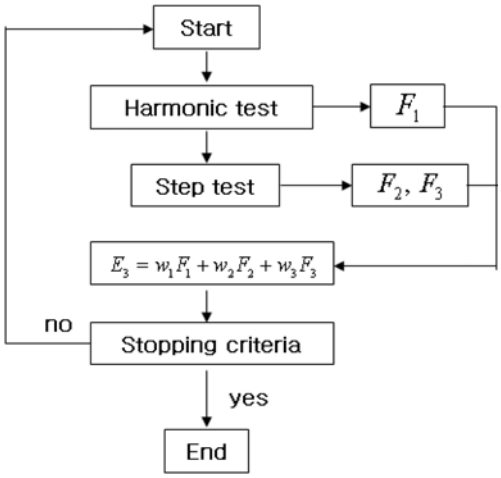

Figure 14. Flow chart of identification through combination of sine and step input.

through step input are shown in Figure 12. The results are in good agreements with experimental results.

To verify the proposed model, the identified results are applied to a sine input with 2.0 mm of displacement and 10 Hz. The bushing forces due to sine input after identification through step input are shown in Figure 13. As shown in Figure 13, the maximum difference between experiment and simulation is 500 N. Thus, the identified results in step input can not be applied to a sine input. Therefore, another identification is required for a combined input of the sine input and step input.

4.3. Combination of Sine and Step Input

Since suspension bushings experience complex excitation input combined with sine and step input simultaneously, a nice model to satisfy the complex excitation input is required. In this section, an identification flow chart to consider these two inputs is developed as shown in Figure 14.

The objective function for the combined input can be written as follows:

$$E_3 = w_1F_1 + w_2F_2 + w_3F_3 \quad (8)$$

where F_1 is the objective function due to sine input and F_2 and F_3 are the objective functions due to step input. The sum of weight factors equals unity as shown the equation (9).

$$w_1 + w_2 + w_3 = 1 \quad (9)$$

where, $w_1 = 0.5$, $w_2 = w_3 = 0.25$.

The characteristics according to the rise time and relaxation phenomenon are considered to represent the response of the step input. In this paper, the weighting factor (w_1) for the rise time is set to 0.5 and the weighting factor for the relaxation phenomenon follows the equation like this: $w_2 + w_3 = 0.5$

Table 5 shows the results of the identification. Bushing forces due to sine input after identification with complex

Table 5. Parameter values obtained from the identification (sine and step input).

Parameter	Opt. value	Parameter	Opt. value
c_o	261.990	c_2	1.691
k_o	2393.280	k_2	5.488
β_1	12.063	β_2	0.837
γ_1	−7.480	γ_2	−4.259
n_1	0.562	n_2	0.951
α_1	1.301	α_2	0.121
c_1	1.485	A_1	2333.745
k_1	2177.470	A_2	32.510

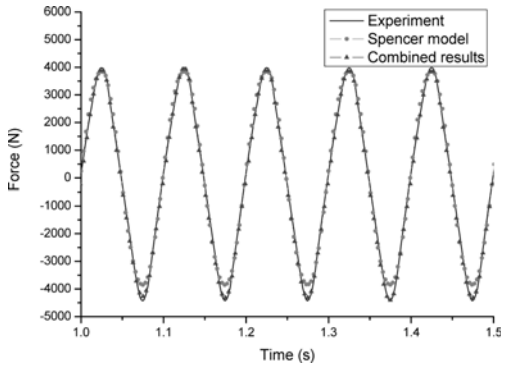

Figure 15. Bushing forces due to sine input after identification due to complex inputs.

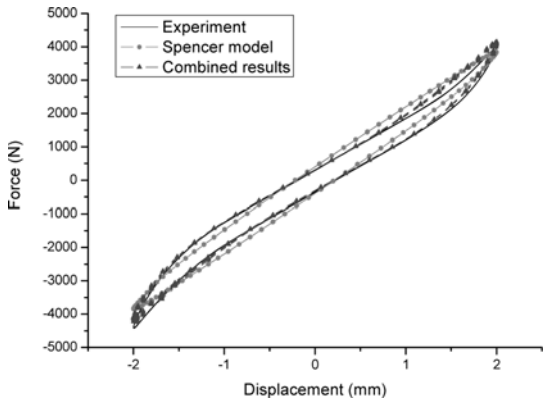

Figure 16. Bushing forces vs. displacements due to sine input between the Spencer's and proposed model.

inputs are shown in Figures 15 and 16.

Figures 15~17 show the comparisons between the Spencer model and the proposed model. As shown in Figures 15 and 16, the Spencer model has a 540 N (12.2%) difference from the results of the experiments. The maximum difference occurs when the bushing is about to be compressed. In experiments, the pinching phenomenon increases when the bushing displacement is over ± 1.0 mm, but the Spencer model can not account for this phenomenon. However, in the case of the combined identification, the maximum

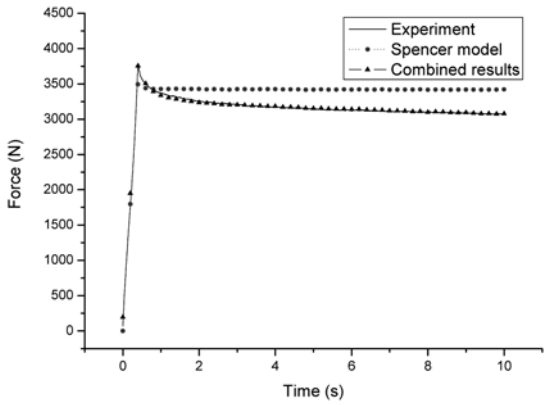

Figure 17. Bushing forces due to step input between the Spencer's and proposed model.

difference between the experimental values and the simulation values is reduced to 194 N (4.4%). In addition, the pinching phenomenon and nonlinear characteristics are represented accurately. As shown in Figure 17, when the time is 0.4 s, the Spencer model and the proposed model have differences of 250 N (6.6%) and 8 N (0.2%), respectively, when compared to experiments. When the time is 10 s, the Spencer model and the proposed model have differences of 350 N (11.4%) and 44 N (1.4%), respectively. Therefore, the proposed model better predicts the relaxation phenomenon due to step input compared to Spencer model.

5. VERIFICATION OF PROPOSED MODEL

5.1. Error Analysis

A dynamic analysis was carried out to verify the proposed bushing model. A dynamic bushing model is generated by using the user routine in the ADAMS/VIEW and bushing forces is calculated by using the SFORCE in the ADAMS/VIEW. The sine and step inputs as shown in the previous section are used to investigate the errors due to frequency and displacement. Frequencies of 1, 10, 20, and 30 Hz and displacements of 0.5, 1.0, 2.0, and 3.0 mm are used. In the step input, rise times of 0.1, 0.2, and 0.4 s and 1.0, 2.0, and 3.0 mm displacements are used. Equation (10) is defined to investigate the errors between the experiments and the simulations. The errors due to sine input are represented in

Table 6. Errors due to sine input. (Unit: %)

Disp. (mm) \ Freq. (Hz)	1	10	20	30
0.5	3.75	7.41	7.73	8.47
1.0	2.22	7.26	7.35	7.92
2.0	0.83	0.31	0.47	2.30
3.0	3.38	2.70	3.96	5.17

Table 7. Errors due to step input. (Unit: %)

Disp. (mm) \ Rise time (s)	0.1	0.2	0.4
0.5	3.75	7.41	7.73
1.0	2.22	7.26	7.35
2.0	0.83	0.31	0.47
3.0	3.38	2.70	3.96

Table 6 and the errors due to step input are shown in Table 7.

$$E_3 = \frac{|RMS(F_{\exp}) - RMS(F_{pre})|}{RMS(F_{\exp})} \quad (10)$$

The smallest error is produced when the input with 10 Hz and 2.0 mm displacement is imposed on the bushing. This is because the input with 10 Hz and 2.0 mm displacement is used for the identification process. The higher the frequency, the more the error increases. This is because when the frequency is higher, the slope of the bushing forces versus displacements increases. As shown in Figure 3, when the excitation displacement is over 1.0 mm, the pinching phenomenon occurs. In the parameter identification process, the proposed model is supposed to well represent the pinching phenomenon. Therefore, for less than 1.0 mm excitation input, the error may increase a little bit.

5.2. Verification with Random Input

To validate the proposed model, the random input is imposed on the bushing. In Table 7, when the excitation input is 3.0 mm displacement, the error between experiment and proposed model is less than 4%. The random input less than 2.0 mm displacement with index 'n = 2.5' is applied to the proposed bushing model.

As shown in Figures 18 and 19, the bushing forces obtained with the proposed model are in good agreements. During the initial few time steps, there are small differences between experiments and simulations. However, the simulation results show good agreement with experiments in the overall range. Although the parameter identification

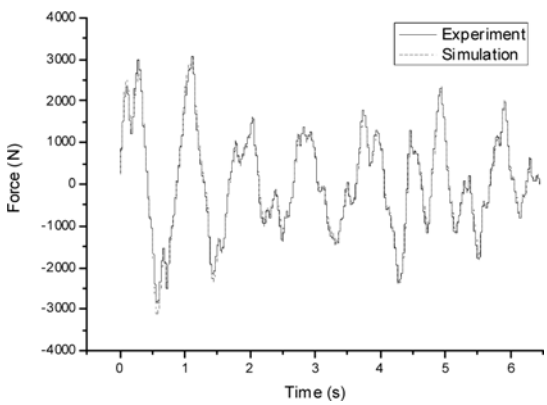

Figure 18. Forces vs. time (random excitation).

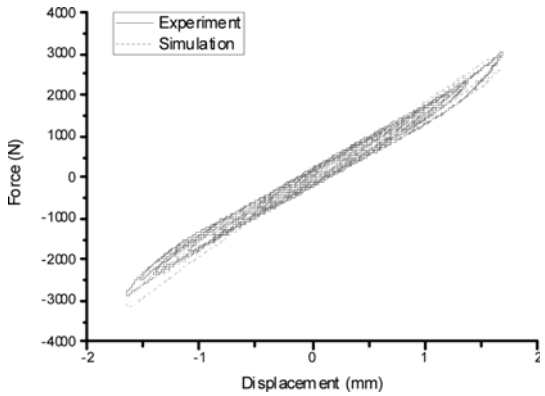

Figure 19. Force vs. displacement (random excitation).

was carried out using the deterministic functions such as sine and step inputs, the responses from the random inputs are almost identical to the experiments. This shows that the proposed model can be realized as the bushing model for the vehicle dynamics simulation.

6. CONCLUSIONS

In this paper, the Bouc-Wen hysteretic differential model is employed and modified to generate the rubber bushing model. The rubber bushing characteristics were tested by using a MTS 3-axis rubber tester. Sine wave, step input, and random excitations are imposed on the bushing. The ADAMS program is used to generate the Bouc-Wen hysteretic bushing model. The VisualDOC program is employed to find the optimal parameters for bushing model. An error function is defined to find optimal parameters of the model. The parameter identification is carried out to satisfy the static and dynamic characteristics due to sine and step excitation inputs.

It is observed that the proposed model can predict the bushing forces under sine, step, and random inputs well. The errors are within 10% in the overall range. To show the fidelity of the proposed model, a numerical example was carried out. Although the parameter identification was performed using the sine and step inputs, the responses from the random inputs are almost identical to the experiments over the whole range. In addition, it is easy to generate the proposed model using the characteristic results from the sine and step inputs. Therefore, the proposed bushing model can be used as the bushing model for the vehicle dynamics simulation. For a practical bushing model, the 3-axis Bouc-Wen bushing model will be developed in the future.

ACKNOWLEDGEMENT−This work was supported by the Ministry of Commerce, Industry and Energy (MOCIE) of Korea for its financial support (grant 10024232-2007-21).

REFERENCES

Atkinson, K. E. and Han, W. (2004). *Elementary Numerical Analysis.* John Wiley & Sons. NJ. 2271−2298.

Blundell, M. V. (1998). The influence of rubber bush compliance on vehicle suspension movement. *Materials and Design*, **19**, 29−37.

Bouc, R. (1967). Forced vibration of mechanical systems with hysteresis. *Proc. 4th Int. Conf. Nonlinear Oscillations*. Czechoslovakia. 315−315.

FunctionBay, Inc. (2006). *RecurDyn Theoretical Manual Ver. 6.1*. Korea.

MSC Software Corporation (2005). *ADAMS User's Manual*. USA.

Ni, Y. Q., Ko, J. M. and Wong, C. M. (1998). Identification of non-linear hysteretic isolators from periodic vibration tests. *J. Sound and Vibration* **217**, **4**, 737−756.

Ok, J. K., Sohn, J. H., Lee, S. K., Park, S. J. and Yoo, W. S. (2005), Bushing model for vehicle dynamics analysis using Bouc-Wen hysteretic model. *Proc. IDETC 2005*, Long Beach, CA., 1−6.

Ok, J. K., Yoo, W. S. and Sohn, J. H. (2007). Experimental study on the bushing characteristics under several excitation inputs for bushing modeling. *Int. J. Automotive Technology* **8**, **4**, 455−465.

Sain, P. M., Sain, M. K., Spencer, B. F. and Dain, J. D. (1998). The Bouc hysteresis model: An initial study of qualitative characteristics. *Proc. American Control Conf.,* 2559−2563.

Spencer, B. F., Dyke, S. J., Sain, M. K. and Carlson, J. D. (1997). Phenomenological model for magnetorheological dampers. *J. Engineering Mechanics*, *ASCE* **123**, **3**, 230−238.

Sues, R. H., Mau, S. T. and Wen, Y. K. (1988). System identification of degrading hysteresis restoring forces. *J. Engeering Mechanics*, *ASCE* **114**, **5**, 833−846.

Vanderplaats Research & Development, Inc. (2006). *VisualDOC 6.0 Users Manual*. USA.

Wen, Y. K. (1975). Approximate method for nonlinear random vibration. *J. Engineering Mechanics Division*, *ASCE* **101**, **4**, 249−264.

Yoo, W. S., Baek, W. K. and Sohn, J. H. (2004). A practical model for bushing components for vehicle dynamic analysis. *Int. J. Vehicle Design* **36**, **4**, 345−364.